



**Bell correlations of a thermal fully connected spin chain in the vicinity of a quantum critical point**Danish Ali Hamza  and Jan Chwedeńczuk *Faculty of Physics, University of Warsaw, ulica Pasteura 5, PL-02-093 Warsaw, Poland*

(Received 21 March 2024; revised 23 May 2024; accepted 28 June 2024; published 11 July 2024)

Bell correlations are among the most exotic of the phenomena through which quantum mechanics manifests itself. Their presence signals that the system may violate the postulates of local realism—conjectures once thought to be to be a non-negotiable property of the physical world. The importance of Bell correlations from this fundamental point of view is even further clarified by their applications, ranging from quantum cryptography to quantum metrology and quantum computing. It is therefore of growing interest to characterize the “Bell content” of complex, scalable many-body systems. Here, we perform a detailed analysis of the character and strength of many-body Bell correlations in interacting multiqubit systems with particle exchange symmetry. Such a configuration can be described by an effective Schrödinger-like equation, which allows precise analytical predictions. We show that in the vicinity of the quantum critical point, these correlations quickly become so strong that only a fraction of the qubits remain uncorrelated. We also identify the threshold temperature above which thermal fluctuations destroy Bell correlations. We hope that the approach presented here, due to its universality, will be useful for upcoming research on genuinely nonclassical Bell-correlated complex systems.

DOI: [10.1103/PhysRevA.110.012210](https://doi.org/10.1103/PhysRevA.110.012210)**I. INTRODUCTION**

In their 1935 paper [1] Einstein, Podolsky, and Rosen (EPR) suggested that quantum mechanics should be complemented by a local and realistic theory [1]. In 1964 Bell showed that such an extension of quantum mechanics cannot exist. The argument against local realism uses the simplest nontrivial many-body system: two spin-1/2 particles [2]. Despite its deceptive simplicity, for many years this system has driven the progress of both theory and experiment. In 1969, the Clauser-Horne-Shimony-Holt inequality [3], which refined Bell’s formulation, paved the way for the first experiments showing the violation of Bell inequalities [4–15]. Finally, a loophole-free test of Bell nonlocality was reported [16], rejecting local realism in quantum mechanics. The importance of these efforts was recognized by the Nobel committee in 2022.

With the advent of noisy intermediate-scale quantum (NISQ) devices, research interest has shifted to more complex systems. It has become increasingly important to understand how fundamental quantum relations, such as entanglement [17,18], EPR steering [1,19,20], and Bell nonlocality, can be created, especially in multiqubit systems. These highly nonclassical correlations are of particular importance for measurement-based quantum computing (MBQC) [21–25], for which entanglement or Bell correlations of the type discussed here are a necessary computational resource for the input state [26,27].

The problem of detecting many-body Bell correlations, which are the main focus of this work, has been formulated for  $N$ -qubit systems using  $N$ -body correlation functions in various ways, most notably by means of Mermin-Bell inequalities [28]. In this work we rely on the formulation of Bell inequalities from Refs. [29–31]. It enabled us to establish the link between the Bell nonlocality and quantum-enhanced

metrology [32] and to determine the strength of many-body Bell correlations in the commonly used method of creating atomic spin-squeezed states [33,34], i.e., the one-axis twisting method [35–41].

Bell correlations in many-body systems have been the subject of recent theoretical and experimental research, mostly on atomic systems. In Ref. [42] a method for the certification of such correlations using two-body observables was proposed. For bosonic systems, it takes an experimentally friendly form that allows for direct verification by measuring the two lowest moments of the angular momentum operators describing a two-mode Bose-Einstein condensate (BEC) [43]. Subsequently, this method was used to confirm Bell correlations in two-mode BECs in the ground and thermal states [44].

The present work takes a step forward by adapting the correlation order to the number of qubits, thus focusing on many-body Bell correlations. We study the emergence of Bell correlations in the versatile and scalable multiqubit system. This is a collection of  $N$  qubits in which the interactions of all the pairs are of equal strength. This setup can be realized using different platforms well suited for quantum technologies, such as the fully connected Ising spin chain [45–52], or, alternatively, by trapping the BEC in a double-well potential. While we will refer to the latter case throughout this work, it is equivalent to the former from the perspective of the problems considered here. In this scenario, the separated single-body states localized around the two minima of the trap play the role of a pair of single-qubit levels. In the tight-binding regime, this system is described by the Bose-Hubbard (BH) Hamiltonian, in which the on-site two-body interactions compete with the coherent Josephson tunneling across the barrier of the double-well potential [53–59]. On the attractive side of the interaction, there is a quantum phase transition (QPT) [60–70], at which point the properties of the BH Hamiltonian suddenly change—from a Gaussian state to the macroscopic

superposition [62–67]. We show that in the vicinity of this point, the Bell correlations are genuinely many body; i.e., a macroscopic fraction of the qubits are Bell correlated. To show this, we derive a simple, but informative, formula that allows us to predict the strength of Bell correlations associated with this emergent macroscopic superposition. We then consider nonzero temperatures and analytically demonstrate that the relevant temperature scale, above which the thermal fluctuations destroy the Bell nonlocality, is related to the energy gap between the ground state and the first excited state. This allows us to derive a clear criterion for the threshold, from the point of view of many-body Bell correlations: temperature. We also carry out a numerical study of the effect of fluctuations of the energy imbalance between the two modes.

The MBQC can use the states with large components of the density matrix which are related to the Greenberger-Horne-Zeilinger (GHZ) coherence [27]. As we argue in Sec. III, when this type of superposition is big, it leads to the violation of the many-body Bell inequality. We precisely characterize the multiqubit states from this point of view, hopefully contributing to the field of MBQC and allowing for accurate planning of future experiments.

## II. MANY-BODY QUANTUM SYSTEMS

Consider a collection of  $N$  qubits (spin-1/2 particles) fully connected via the distance-independent two-body interaction of strength  $U$ . The spins are subject to an external uniform magnetic field aligned by the  $x$  axis, whose amplitude is proportional to  $\Omega$ . One possibility of modeling such a system is via the Ising model, the one on which we focus in this work. The Hamiltonian reads

$$\hat{H} = -\Omega \sum_{i=1}^N \hat{\sigma}_x^{(i)} + \frac{U}{2} \sum_{i \neq j=1}^N \hat{\sigma}_z^{(i)} \hat{\sigma}_z^{(j)}. \quad (1)$$

Here,  $\hat{\sigma}_\xi^{(k)}$  is the  $\xi$  component of the triad of Pauli matrices for the  $k$ th spin (i.e.,  $\xi = x, y, z$ ). Note that this Hamiltonian is invariant under the exchange of any pair of spins; hence, all its eigenstates possess this symmetry. Thus, to analyze the many-body properties of the ground and the thermal states, it is convenient to map it onto the bosonic BH Hamiltonian in the tight-binding limit, namely,

$$\hat{H}_{\text{bh}} = -\Omega \hat{J}_x + U \hat{J}_z^2, \quad (2)$$

where the collective spin operators are

$$\hat{J}_\xi = \frac{1}{2} \sum_{k=1}^N \hat{\sigma}_\xi^{(k)}. \quad (3)$$

The spectrum of this operator is spanned by the symmetrized states  $|N-n, n\rangle$  of  $n$  spins in the  $-1$  eigenstate of, for instance, the  $z$ -component Pauli operators and the remaining  $N-n$  spins in the  $+1$  eigenstate. Hence, the dimensionality of the symmetric subspace  $\mathcal{H}_N^{(\text{sym})}$ , compared to the size of the whole Hilbert space  $\mathcal{H}_N$ , is

$$\dim \mathcal{H}_N^{(\text{sym})} = N+1 \quad \text{vs} \quad \dim \mathcal{H}_N = 2^N. \quad (4)$$

Therefore, any state vector  $|\psi\rangle$  in  $\mathcal{H}_N^{(\text{sym})}$  can be expressed as

$$|\psi\rangle = \sum_{n=0}^N \psi_n |N-n, n\rangle, \quad \sum_{n=0}^N |\psi_n|^2 = 1. \quad (5)$$

To extract the crucial properties of the eigenstates of the Hamiltonian from Eq. (2) we follow the steps in Ref. [71]. First, we project the stationary Schrödinger equation onto the  $n$ th element of the basis, i.e.,  $\langle N-n, n | \hat{H} | \psi \rangle = E \psi_n$ , giving

$$-\frac{\Omega}{2} [\psi_{n+1} \sqrt{(N-n)(n+1)} + \psi_{n-1} \sqrt{(N-n+1)n}] + \frac{U}{4} (N-2n)^2 \psi_n = E \psi_n. \quad (6)$$

Next, we introduce the normalized population imbalance,

$$z_n = \frac{(N-n) - n}{N} = 1 - \frac{2n}{N}, \quad (7)$$

which varies from  $-1$  to  $1$ , with the increment equal to  $\Delta z = 2/N$ . Equation (6) expressed in terms of this new variable  $z_n$  becomes

$$-\frac{\Omega N}{2} [\psi_{n+1} f_+(z_n) + \psi_{n-1} f_-(z_n)] + \frac{UN^2}{4} \psi_n z_n^2 = E \psi_n, \quad (8)$$

$$f_{\pm}(z_n) = \sqrt{\frac{1 \pm z_n}{2} \left( \frac{1 \mp z_n}{2} + \frac{1}{N} \right)}.$$

When  $N$  is large, the  $1/N$  term in  $f_{\pm}$  can be neglected. Furthermore, as the increment of  $z_n$  diminishes, the discrete variable can be approximated with a continuous  $z$ . In particular, this means that the finite difference tends to

$$\frac{\psi_{n+1} + \psi_{n-1} - 2\psi_n}{(\Delta z)^2} \approx \frac{d^2}{dz^2} \psi(z). \quad (9)$$

In such a large- $N$  regime we obtain a stationary one-dimensional (1D) Schrödinger-like equation for a fictitious unit-mass particle subject to an external potential,

$$V_{\text{eff}}(z) = -\sqrt{1-z^2} + z^2 \gamma / 2, \quad (10)$$

with  $\gamma = UN/\Omega$ , i.e.,

$$\left( -\frac{2}{N^2} \sqrt{1-z^2} \frac{d^2}{dz^2} + V_{\text{eff}}(z) \right) \psi(z) = \tilde{E} \psi(z). \quad (11)$$

The normalized energy is  $\tilde{E} = \frac{2E}{\Omega N}$ . Note also that here,  $2/N$  is the dimensionless equivalent of the reduced Planck's constant  $\hbar$ . For the mathematical details of this derivation with a discussion of all its limitations, we refer readers to Ref. [71].

The ground state of Eq. (11) depends crucially on the value of  $\gamma$  and hence on the ratio (and the sign) of the interaction-to-tunneling energies. For large and positive  $\gamma$ 's,  $V_{\text{eff}}(z) \approx \frac{1}{2} \gamma z^2$ ; hence, the problem simplifies to that of the 1D harmonic potential. As  $\gamma$  grows, the width of the ground-state Gaussian shrinks. This implies diminishing fluctuations of the population imbalance, which, since the intramode coherence is mostly maintained, signals the spin squeezing of the state [33,34].

On the negative- $\gamma$  side, the shape of the ground state is more diversified, depending on the value of the parameter. For  $\gamma \gtrsim \gamma_0 \equiv -1$  the wave function is still a Gaussian, but

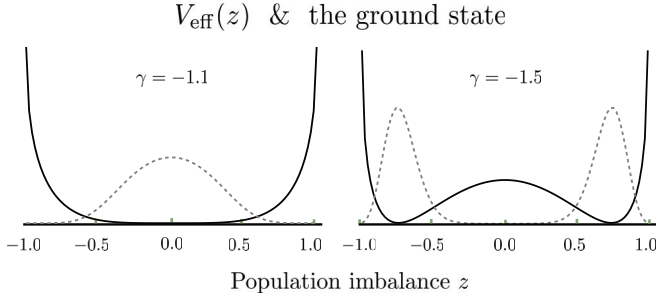


FIG. 1. The effective potential  $V_{\text{eff}}(z)$  (solid black lines) for  $N = 100$  and  $\gamma = -1.1$  (left) and  $\gamma = -1.5$  (right). The dashed gray lines show the ground state for each case.

now its width grows as  $\gamma$  approaches  $\gamma_0$ ; this, in turn, signals the phase squeezing of the sample [72]. However, when  $\gamma_0$  is crossed,  $V_{\text{eff}}(z)$  changes abruptly, indicating the passage through the QPT. Upon crossing this point, the fluctuations of the population imbalance grow rapidly, more sharply for higher  $N$  (see Fig. 4 of Ref. [71] and the discussion therein). This is a consequence of the buildup of a macroscopic superposition when qubits symmetrically occupy the two modes. This effect is visualized in Fig. 1, where we show how the potential and the ground state change across this highlighted point. Upon crossing  $\gamma_0$ , the potential breaks and develops two minima at positions  $\pm z_0$ , with  $z_0 = (1 - 1/\gamma^2)^{1/2}$ . A quantum state that respects the left-right symmetry of the problem is a macroscopic superposition of two separated wave packets. As  $\gamma \rightarrow -\infty$ , the maxima of  $\psi(z)$  separate, tending towards the NOON state, which in the ket notation used in Eq. (5) is  $|\psi\rangle = 1/\sqrt{2}(|N, 0\rangle + |0, N\rangle)$ . A similar transition is present in nonsymmetric spin chains, as discussed in Sec. VI. As we argue in the following section, the emergence of this twin-peak structure is a signature of strong Bell correlations, and their analysis is the main focus of this work.

The shape of the potential after the breaking suggests that some of the properties of the state vector can be extracted by locally approximating  $V_{\text{eff}}(z)$  with two harmonic oscillators located at  $\pm z_0$ , namely (recall that the fictitious particle has a mass set to unity),

$$V_{\text{eff}}(z) \simeq \frac{1}{2}\omega^2(z \pm z_0)^2 + V_0, \quad (12)$$

where  $\omega = \sqrt{\gamma(1 - \gamma^2)}$  and  $V_0 = -\frac{\gamma^2+1}{\gamma}$ . In Fig. 2 we show how this approximation works for  $N = 500$  qubits and  $\gamma = -1.4$ . Roughly speaking, the position of the lowest-lying levels, denoted by the horizontal blue dashed line, seems to be deep in the regime where the approximation is valid. Nevertheless, this must be analyzed in more detail, as discussed below.

Note that the harmonic potential (12) is an approximation of the already approximate model of the Schrödinger-like equation in Eq. (11). In order to make sure that in this process the errors do not accumulate to some unacceptable level, we perform the exact diagonalization of the BH Hamiltonian from Eq. (2) and compare its two lowest-lying energy levels with those from the harmonic approximation [HA; see Eq. (12)]. In Fig. 3 we show the normalized energy difference between these two outcomes, expressed as a percentage,

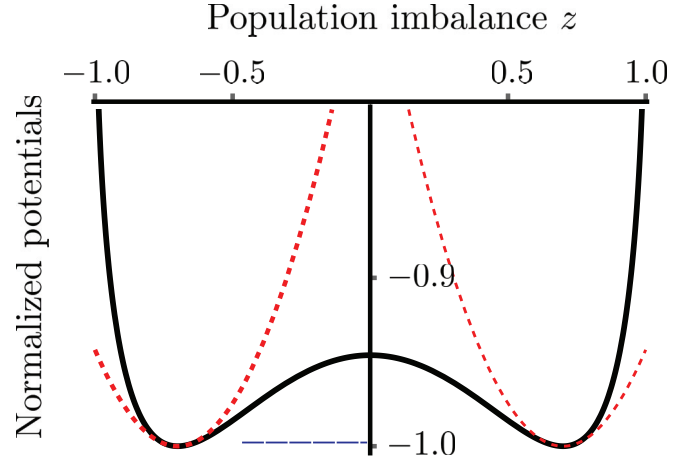


FIG. 2. Comparison of the potentials  $V_{\text{eff}}(z)$  (normalized to  $V_{\text{min}} = -1$ ) from Eqs. (10) and from (12) for  $N = 500$  and  $\gamma = -1.4$ . The horizontal dashed blue line shows the energy scales of the few lowest-lying states of either potential.

namely,

$$\Delta E_i = \left| \frac{E_i^{(\text{BH})} - E_i^{(\text{HA})}}{E_i^{(\text{BH})}} \right| \times 100\% \quad (13)$$

for  $i = 0$  (ground state) and  $i = 1$  (first excited state). The left panel shows the difference for two  $\gamma$ 's equal to  $-1.1$  and  $-1.5$  as a function of  $N$ . As expected from the procedure described above, the discrepancy diminishes as  $N$  grows and for  $N = 500$  can be safely kept below 1%. Similarly, the variation of  $\gamma$  for fixed  $N$ 's (100 and 500; see the right panel) confirms the satisfactory precision of the harmonic approximation. Last, but not least, we scrutinize the quality of the harmonic approximation by calculating the overlap between the eigenstates corresponding to these two energy levels with the eigenstates of the exact BH Hamiltonian,

$$\mathcal{F}_i = |\langle \psi_i^{(\text{BH})} | \psi_i^{(\text{HA})} \rangle|^2 \times 100\%, \quad (14)$$

again with  $i = 0, 1$ . In Fig. 4 we show that for the ground state, the fidelity  $\mathcal{F}_0$  is above 90% for a wide range of  $\gamma$ 's and  $N$ 's. While the fidelity  $\mathcal{F}_1$  can be unsatisfactory for smaller  $N$ 's and in the direct vicinity of the QPT, we will argue that even for  $T \neq 0$  this is not a concern—the Bell correlator we discuss

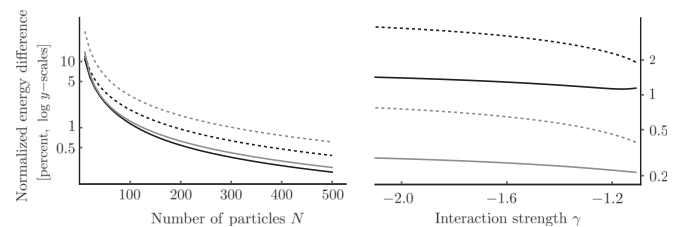


FIG. 3. Left: The normalized energy difference  $\Delta E_i$  [see Eq.(13)] for  $i = 0$  (the ground state, solid lines) and  $i = 1$  (the first excited state, dashed lines) of the potentials (10) and (12) for  $\gamma = -1.1$  (black) and  $\gamma = -1.5$  (gray) as a function of  $N$ . Right: Here,  $N$  is fixed to  $N = 100$  (black) and  $N = 500$  (gray) while  $\gamma$  is varied.

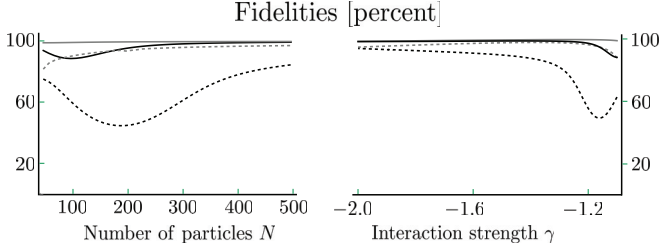


FIG. 4. The quality of the harmonic approximation quantified by the fidelity  $\mathcal{F}_i$  of the ground and first excited states, expressed as a percentage [see Eq. (14)]. The left panel displays  $\mathcal{F}_i$  as a function of the number of particles  $N$  for  $\gamma = -1.1$  (black) and  $\gamma = -1.5$  (gray). The right panel is the reverse: here,  $N$  is fixed to 100 (black) and 500 (gray) while  $\gamma$  changes.

below is mostly characterized by the properties of the ground state.

In this section we have shown how to replace the exact quantum BH model with an approximate twin-harmonic approximation. It is valid on the negative side of the quantum critical point and will be our workhorse for the derivation of simple, yet powerful, analytical formulas of the many-body Bell correlations.

### III. MANY-BODY BELL CORRELATOR

We now briefly review the theory behind the method of detecting many-body Bell correlators that will be used in this work. For an extensive discussion of its properties, see Refs. [30,73–76].

Consider  $m$  objects, each being a subject of local measurements of two binary quantities [77],  $\sigma_x^{(k)} = \pm 1$  and  $\sigma_y^{(k)} = \pm 1$ , with  $k = 1, \dots, m$ . These outcomes are combined locally (i.e., separately for each object) into  $\sigma_+^{(k)} = \frac{1}{2}(\sigma_x^{(k)} + i\sigma_y^{(k)})$ , and the following correlator is constructed:

$$\mathcal{E}_m = |\langle \sigma_+^{(1)} \cdots \sigma_+^{(m)} \rangle|^2. \quad (15)$$

Here,  $\langle \cdot \rangle$  denotes averaging over experimental repetitions. If  $\mathcal{E}_m$  can be reproduced by a system that is consistent with the local hidden-variable theory [1,2,78,79], then this average can be expressed in terms of an integral over this (possibly multivariate) variable  $\lambda$  distributed with a probability density  $p(\lambda)$ , namely,

$$\mathcal{E}_m = \left| \int d\lambda p(\lambda) \sigma_+^{(1)}(\lambda) \cdots \sigma_+^{(m)}(\lambda) \right|^2. \quad (16)$$

Using the Cauchy-Schwarz inequality for complex integrals, we obtain

$$\mathcal{E}_m \leq \int d\lambda p(\lambda) |\sigma_+^{(1)}(\lambda)|^2 \cdots |\sigma_+^{(m)}(\lambda)|^2 = 2^{-m}. \quad (17)$$

Thus,  $\mathcal{E}_m \leq 2^{-m}$  is the  $m$ -body Bell inequality. Note that each party has the freedom of choice of the orientations of its operator  $\hat{\sigma}$  in Eq. (15). The most general  $N$ -qubit Bell inequality, taking into account all possible choices at once, was formulated in [80].

This inequality can be tested with quantum systems of  $m$  qubits. In this case, the correlator  $\mathcal{E}_m$  from Eq. (15) is replaced

by its quantum-mechanical ( $q$ ) equivalent

$$\mathcal{E}_m^{(q)} = |\text{Tr}[\hat{\rho} \hat{\sigma}_+^{(1)} \otimes \cdots \otimes \sigma_+^{(m)}]|^2. \quad (18)$$

For the case of the  $m$ -qubit GHZ state [81], i.e.,

$$|\psi\rangle = \frac{1}{\sqrt{2}}(|\uparrow\rangle^{\otimes m} + |\downarrow\rangle^{\otimes m}), \quad \hat{\sigma}_+|\downarrow\rangle = |\uparrow\rangle, \quad (19)$$

we obtain  $\mathcal{E}_m^{(q)} = 1/4$ , hence the exponential (as a function of  $m$ ) breaking of the bound (17).

This quantum correlator (18) can be adapted to symmetric systems, in which only collective operations are allowed. In this case, the single-body particle-resolving operators  $\hat{\sigma}_+^{(k)}$  are replaced with their (still one-body) collective equivalent

$$\hat{\sigma}_+^{(k)} \longrightarrow \hat{J}_+ = \sum_{k=1}^N \hat{\sigma}_+^{(k)}, \quad (20)$$

in analogy to Eq. (3). Upon replacing the  $\sigma_+^{(k)'}$ s in Eq. (18) by  $\hat{J}_+^m$  one notices that there are  $N!/(N-m)!$  more terms in the latter case, which is a consequence of the permutational invariance of the problem. Hence, the proper symmetric (the symmetrization is here denoted by the tilde symbol)  $m$ -body Bell inequality is

$$\tilde{\mathcal{E}}_m^{(q)} \equiv |\langle \hat{J}_+^m \rangle|^2 \leq \left( \frac{N!}{(N-m)!} \right)^2 2^{-m}, \quad (21)$$

and more details on its derivation can be found in Ref. [76]. It is convenient to normalize the left-hand side of this inequality by its right-hand side and introduce [82]

$$Q_m = \log_2 \left[ 2^m \left( \frac{N!}{(N-m)!} \right)^{-2} \tilde{\mathcal{E}}_m^{(q)} \right]. \quad (22)$$

The Bell inequality then becomes

$$Q_m \leq 0. \quad (23)$$

It is the purpose of the remainder of this work to demonstrate that both at zero temperature ( $T = 0$ ) and when  $T > 0$ , there exists an order  $m = \mu$  of the Bell correlator which is significantly above the nonlocality bound  $Q_\mu > 0$  in the vicinity of the QPT. This particular  $Q_\mu$ , as we argue below, means that an extensive (i.e., growing linearly with  $N$ ) number of qubits are Bell correlated. Moreover,  $Q_\mu$  turns out to be directly linked to how far  $\gamma$  is from the quantum critical point. Benefiting from the above-verified harmonic approximation, we will connect the correlation order  $\mu$  and the value of the corresponding correlator  $Q_\mu$  with  $\gamma$  using a simple, but versatile, analytical formula and extend the analysis to nonzero temperatures.

The concept relies on the following observation. If the operator  $\hat{J}_+^m$  that determines the correlator  $Q_m$  acts on a ket  $|N-n, n\rangle$ , it gives

$$\begin{aligned} \hat{J}_+^m |N-n, n\rangle &= j_{nm} |N-n+m, n-m\rangle, \\ j_{nm} &= m! \sqrt{\binom{n}{m} \binom{N-n+m}{m}}. \end{aligned} \quad (24)$$

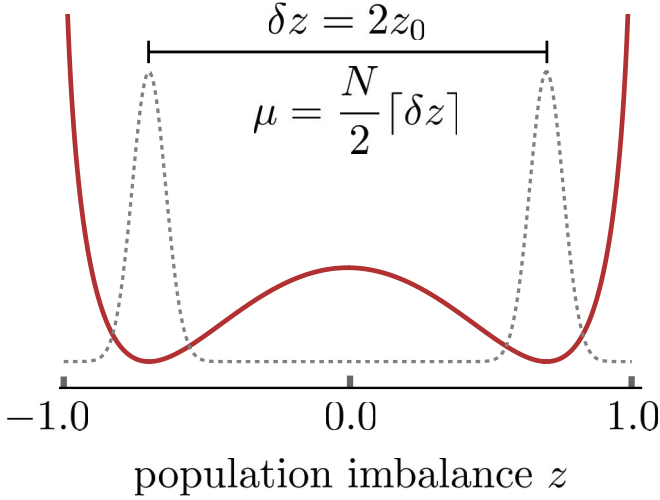


FIG. 5. The ground state of the Bose-Hubbard Hamiltonian and the effective potential  $V_{\text{eff}}(z)$  (both in arbitrary units picked only for illustration) for  $N = 500$  qubits and  $\gamma = -1.4$ . As argued in the text, the distance between the peaks determines the relevant order of the Bell correlator.

Hence, the average of this operator is equal to

$$\langle \hat{J}_+^m \rangle = \sum_{n=0}^{N-m} \varrho_{n,n+m} j_{nm}, \quad (25)$$

i.e., a coherent sum of all the elements of the density matrix distanced by  $m$  from the diagonal and weighted with  $j'_{nm}$ s. Here, we use the general expression for the density matrix in the  $N$ -qubit symmetric subspace, namely,

$$\hat{\varrho} = \sum_{nm'=0}^N \varrho_{nm'} |N-n, n\rangle \langle N-n', n'|. \quad (26)$$

Due to the characteristic twin-peak structure of the ground state, one  $m$  stands out, namely, the one directly linked to the separation of the two maxima  $\delta z = 2z_0$  by means of Eq. (7), i.e.,

$$\mu = \frac{N}{2} [\delta z] = N [z_0] \quad (27)$$

(see Fig. 5). Here,  $[x]$  denotes the integer which is closest to and larger than  $x$  (the “ceil” function). Hence, the following conjecture arises: one particular order of Bell correlator at a given  $\gamma$  stands out, i.e., the one for which  $m = \mu$  holds. Moreover, its value can be reproduced with excellent precision by reducing the sum in Eq. (25) merely to the contribution coming from the peak values at these two maxima positioned at  $n_{\pm} = (N \pm \mu)/2$ . In other words, using Eqs. (21) and (24), the correlator is approximated by

$$Q_{\mu} \simeq \log_2 \left[ 2^{\mu} \left( \frac{N!}{(N-\mu)!} \right)^{-2} |\varrho_{n_+, n_-} j_{n_+, n_-}|^2 \right]. \quad (28)$$

We now show that this very simple formula works exceptionally well for a pure ground state and allows us to determine the threshold temperature, above which the Bell correlator  $Q_{\mu}$  drops below the Bell limit.

It should be underlined that  $Q_{\mu}$  does not provide complete information about Bell nonlocality in the system. At fixed  $\gamma$ , there are various correlation orders that give  $Q_m > 0$  [76]. Also, there are other ways to construct the many-body Bell correlator [80] that, in principle, could yield more information about the nonlocal correlations in this case. Nevertheless, the analysis presented here has two strengths—it is simple, leading to analytical predictions, and it allows us to lower bound the extent of Bell correlations over the system, an important issue for many application aspects, such as quantum-enhanced metrology [32]. We underline that the Bell correlator we use is well suited to detecting the macroscopic superpositions governed by the density-matrix element  $\varrho_{n_+, n_-}$  that forms after the QPT has been crossed (see Fig. 5). Their emergence when  $\gamma \lesssim -1$  is a clear indicator of a rapid growth of Bell correlations, according to Eq. (28).

#### IV. BELL CORRELATIONS AT $T = 0$

The Harmonic approximation indicates the ground state of the system is a superposition of two localized Gaussians, i.e.,

$$|\psi\rangle \simeq \sum_{n=0}^N (C_n^{(+)} + C_n^{(-)}) |N-n, n\rangle, \quad (29)$$

where

$$C_n^{(\pm)} = \left( \frac{\omega}{2\pi N} \right)^{\frac{1}{4}} e^{-\left( \frac{N \pm \mu}{2} - n \right)^2 \frac{\omega}{N}}. \quad (30)$$

Hence, by taking the peak values of the state coefficients [located at  $n_{\pm} = (N \pm \mu)/2$ ] and substituting this result into Eq. (28), we obtain

$$Q_{\mu} = \log_2 \left[ 2^{\mu} \left( \frac{N+\mu}{\mu} \right)^2 \binom{N}{\mu}^{-2} \frac{\omega}{2\pi N} \right]. \quad (31)$$

Keeping the dominant terms that scale with  $N$ , we obtain a simple, but powerful, expression that allows us to lower bound the strength of  $\mu$ -body Bell correlations in the vicinity of the quantum critical point, namely,

$$Q_{\mu} \simeq \mu \log_2 \left[ \frac{N+\mu}{N-\mu} \right] - \mu - N \log_2(\gamma^2). \quad (32)$$

Finally, by using Eq. (27), we obtain the compact formula

$$Q_{\mu} = N f(\gamma), \quad (33)$$

where

$$f(\gamma) = \frac{\sqrt{\gamma^2 - 1}}{|\gamma|} [2 \log_2(\sqrt{\gamma^2 - 1} + |\gamma|) - 1] - 2 \log_2 |\gamma|. \quad (34)$$

Most importantly, the correlator is extensive in  $N$ , which has profound consequences for the quantitative characterization of many-body Bell nonlocality. Moreover, this form of  $Q_{\mu}$  implies that the value of  $\gamma$  at which the many-body Bell correlations emerge is universal (i.e., independent of  $N$ ) and equal to  $\gamma_0 \simeq -1.3$ . The quality of this approximation is shown in Fig. 6, where we plot the ratio of the Bell correlator  $Q_{\mu}$  that is calculated using the exact diagonalization of the Hamiltonian from Eq. (2) to the analytical result from Eq. (32) using

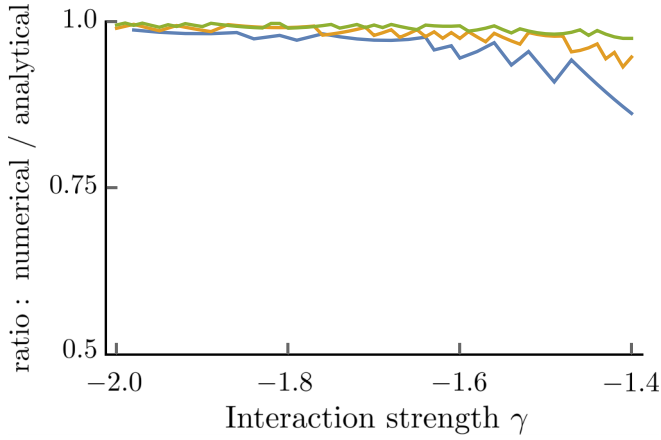


FIG. 6. The ratio of the Bell correlator  $Q_\mu$  obtained from the exact numerical diagonalization of Eq. (2) to the analytical approximation from Eq. (32) for  $N = 200, 500$ , and  $1000$  (from bottom to top) as a function of  $\gamma$ .

$N = 200, 500$ , and  $1000$  qubits. Clearly, the approximation improves for larger  $N$  and with  $\gamma$  farther from the QPT.

Note that the value of  $Q_\mu$  carries information about the nonlocality depth, i.e., about how many qubits are Bell correlated. So if

$$\mu - 2 - (k + 1) < Q_\mu \leq \mu - 2 - k, \quad (35)$$

where  $k \in \mathbb{N}$ , then this correlator can be reproduced with a state of  $m$  qubits, where maximally  $k - 2$  of them are *not* Bell correlated with the rest [75,82,83]. By using Eq. (33) we notice that the depth of Bell correlations in the ground state can be lower bounded because maximally

$$k \leq N[\lceil z_0 \rceil - f(\gamma)] - 2 \quad (36)$$

qubits are not Bell correlated. The description of the relation between the remaining  $M = N - k$  particles, where

$$M \geq N[f(\gamma) - \lceil z_0 \rceil] + 2, \quad (37)$$

requires a model that defies the local realism.

Hence, we conclude that the number of Bell-correlated qubits  $M$  is, universally for all  $N$ , an extensive function of  $N$ , starting from the critical point  $\gamma = \gamma_0$ . This confirms that  $Q_\mu$  is a useful tool to lower bound the nonlocality depth in this system.

## V. QUANTUM CORRELATIONS WITH NOISE

In this section we incorporate two sources of noise that are inevitable in realistic conditions: thermal occupation of excited states and fluctuations of the population imbalance between the two modes.

### A. Thermal noise

First, we calculate the Bell correlator and the nonlocality depth in nonzero temperatures, considering the thermal density matrix

$$\hat{\rho} = \frac{1}{\mathcal{Z}} \sum_n |\psi_n\rangle\langle\psi_n| e^{-E_n\beta}, \quad (38)$$

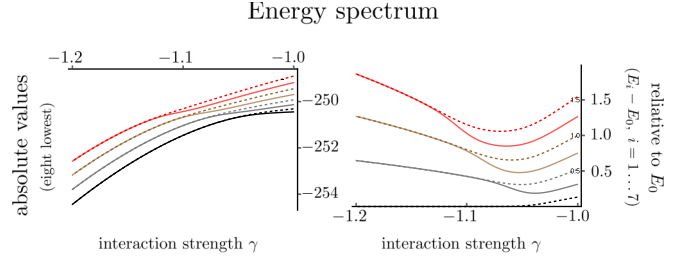


FIG. 7. The energy spectrum (eight lowest levels) of the Hamiltonian  $H_{\text{bh}}$  for  $N = 500$  atoms in the vicinity of the critical point. The left panel shows the energies  $E_i$  ( $i = 0-7$ ), while the right panel displays the seven energy gaps with respect to the ground state  $E_0$ .

where  $\beta^{-1} = k_b T$ ,  $k_b$  is the Boltzmann constant,  $\mathcal{Z}$  is the statistical sum, and  $\hat{H}_{\text{bh}}|\psi_n\rangle = E_n|\psi_n\rangle$ , with the Hamiltonian from Eq. (2).

The characteristic temperature scales are set by the eigenenergies (with respect to the ground state) of the Hamiltonian; hence, first, we plot part of the spectrum for  $\gamma$ 's of interest and  $N = 500$  atoms (see Fig. 7). The energy gaps  $\delta_i = E_i - E_0$  of the seven lowest-lying excited states are all of the order of unity, apart from the first one, i.e.,  $\delta_1$ , which quickly converges to zero upon passing the QPT point. This observation allows us to identify the relevant scale of  $\beta$ 's.

The following toy model indicates that the temperature should be kept well below this smallest gap  $\delta_1$  to retain high values of  $Q_\mu$ . Let us approximate the twin-peak ground state with what is sometimes called a ‘‘Schrödinger’s kitten’’ state,

$$|\psi_0\rangle = \frac{1}{\sqrt{2}} \left( \left| \frac{N+\mu}{2}, \frac{N-\mu}{2} \right\rangle + \left| \frac{N-\mu}{2}, \frac{N+\mu}{2} \right\rangle \right). \quad (39)$$

The gap  $\delta_1$  dropping to zero is the result of the fact that this state is almost degenerate with

$$|\psi_1\rangle = \frac{1}{\sqrt{2}} \left( \left| \frac{N+\mu}{2}, \frac{N-\mu}{2} \right\rangle - \left| \frac{N-\mu}{2}, \frac{N+\mu}{2} \right\rangle \right). \quad (40)$$

Note that this is an approximation of the true ground and first excited states at finite  $\gamma$ , while the exact degeneracy is when  $\gamma \rightarrow \infty$  (i.e., when  $\mu \rightarrow N$ ). Nevertheless, when the temperature is kept sufficiently low that only  $|\psi_0\rangle$  and  $|\psi_1\rangle$  are populated, the thermal density matrix is approximately

$$\hat{\rho} \simeq \frac{1}{1 + e^{-\delta_1\beta}} (|\psi_0\rangle\langle\psi_0| + |\psi_1\rangle\langle\psi_1| e^{-\delta_1\beta}). \quad (41)$$

Substituting this  $\hat{\rho}$  into Eq. (22) gives

$$Q_\mu = \log_2 \left[ 2^\mu \left| \frac{1}{2} \binom{N}{\mu}^{-1} \binom{N+\mu}{\mu} \frac{1 - e^{-\delta_1\beta}}{1 + e^{-\delta_1\beta}} \right|^2 \right]. \quad (42)$$

Clearly, when  $\beta \ll \delta_1$ , i.e., when  $k_b T$  is much larger than the gap, the correlator vanishes. This conjecture is fully confirmed by the exact diagonalization, which gives the thermal state and the correlator  $Q_\mu$  (see the right panel of Fig. 8). Here, the temperature is picked to be equal to 10% of the energy gap  $\delta_1$ , the value of which is calculated using either  $\gamma = -1.1$  (solid black line) or  $\gamma = -1.6$  (solid gray line). The correlator  $Q_\mu$  drops drastically when the interaction strength  $\gamma$  is far away

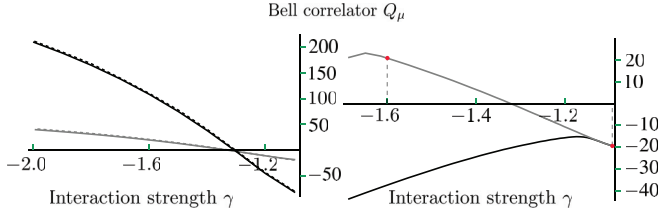


FIG. 8. The Bell correlator calculated with the full Bose-Hubbard Hamiltonian (solid lines) and with the approximate formulas (dashed lines). Left:  $T = 0$  for  $N = 100$  (gray) and  $N = 500$  (black) qubits. The approximate formula is given in Eq. (33). Right: the correlator  $Q_\mu$  calculated with the thermal state [see Eq. (38)] with  $N = 100$  qubits. The black solid line is for  $k_b T_1 = 10\% \times \delta_1$ , which is the gap taken at  $\gamma = -1.1$ . The gray solid line is for  $k_b T_2 = 10\% \times \delta_1$ , where the gap is for  $\gamma = -1.6$ . Hence,  $T_2 < T_1$ . The vertical dashed lines and red dots indicate those values of  $\gamma$ . Clearly, soon after passing these points, when the temperature becomes comparable to the corresponding gap, the correlator drastically drops.

from the QPT, so the population of the excited state becomes significant.

Recall that the many-body Bell correlations detected by  $Q_\mu$  require  $\gamma < -1.3$  [see the discussion below Eq. (33)]. This observation, together with the results from the previous paragraph, yields the threshold temperature, above which the Bell correlations will not be detected by  $Q_\mu$ . Namely, if  $\gamma$  must be below  $\gamma_0$  and the temperature must be at least 1 order of magnitude smaller than the energy gap, the maximal temperature at which  $Q_\mu > 0$  is set by a fraction of the energy gap  $\delta_1$  at  $\gamma_0$ . Since this gap rapidly shrinks with growing  $N$ , we conclude that the higher  $N$  is, the more sensitive the many-body Bell correlator  $Q_\mu$  is to any thermal excitations.

### B. Fluctuations of population imbalance

We now focus on another source of noise, the origin of which is the nonvanishing population imbalance between the two modes [44]. This effect is represented by the addition of the population imbalance operator to Eq. (2), giving the Hamiltonian in units of  $\Omega$ ,

$$\hat{H}_{\text{bh}}^{(\delta)} = -\hat{J}_x + \frac{\gamma}{N} \hat{J}_z^2 + \delta \hat{J}_z, \quad (43)$$

where  $\delta$  is a constant. The population imbalance fluctuates incoherently between experimental realizations, effectively introducing noise into the system. Denoting a ground state of the Hamiltonian (43) as  $|\psi_0^{(\delta)}\rangle$ , a good model of a state that incorporates this noise is

$$\hat{\rho}_{\text{imb}} = \int_{-\infty}^{\infty} d\delta p(\delta) |\psi_0^{(\delta)}\rangle \langle \psi_0^{(\delta)}|, \quad (44)$$

where  $p(\delta)$  is the probability distribution of the random variable  $\delta$ . We model the noise fluctuations with a Gaussian  $p(\delta)$  and numerically calculate the Bell correlator  $Q_\mu$ . The result is shown in Fig. 9 for  $N = 100$  and  $\sigma = 0, 8 \times 10^{-5}, 3 \times 10^{-4}$ , and  $3 \times 10^{-3}$  in units of  $\Omega$ , using four values of the mean population imbalance, namely,  $\langle \delta \rangle = 0$  [Fig. 9(a)],  $\langle \delta \rangle = 10^{-10}$  [Fig. 9(b)],  $\langle \delta \rangle = 10^{-8}$  [Fig. 9(c)], and  $\langle \delta \rangle = 10^{-6}$  [Fig. 9(d)]. Naturally, the effect is more pronounced for higher  $\sigma$ 's and

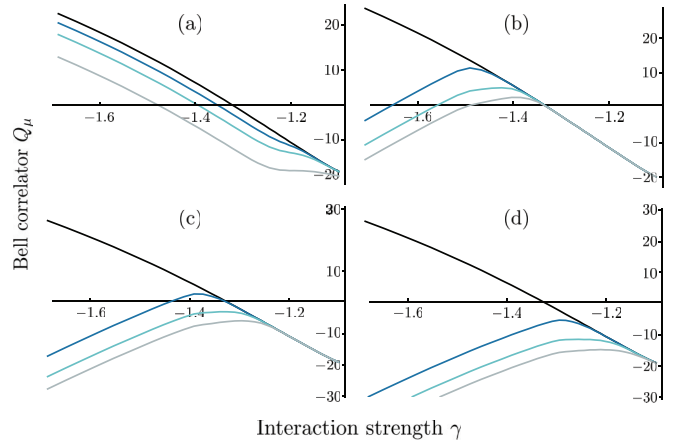


FIG. 9. The Bell correlator  $Q_\mu$  as a function of  $\gamma$  for  $N = 100$  and for four values of the population-imbalance noise width:  $\sigma = 0, 8 \times 10^{-5}, 3 \times 10^{-4}, 3 \times 10^{-3}$ . The higher the value of  $\sigma$  is, the lower lying the curve is. The four panels correspond to the mean population imbalance equal to (a)  $\langle \delta \rangle = 0$ , (b)  $\langle \delta \rangle = 10^{-10}$ , (c)  $\langle \delta \rangle = 10^{-8}$ , and (d)  $\langle \delta \rangle = 10^{-6}$ .

bigger mean population imbalances. We stress that even for a minuscule  $\sigma$  or any  $\langle \delta \rangle \neq 0$ , when  $\gamma \rightarrow -\infty$ , the Bell correlations of all orders will vanish. The reason is that when the interaction energy becomes very large and negative, even a small population imbalance forces qubits to occupy the mode with the lower energy and form a fully separable state of either  $|N, 0\rangle$  or  $|0, N\rangle$ . Nevertheless, our analysis reveals that in the vicinity of the QPT, the many-body Bell correlations of lower orders prevail in the presence of fluctuating population imbalance.

## VI. DISCUSSION AND CONCLUSION

In this work we analyzed the character of the many-body Bell correlations in interacting multiqubit systems with particle-exchange symmetry, such as the fully connected Ising model in a perpendicular magnetic field and the tight-binding Bose-Hubbard Hamiltonian of a Bose-Einstein condensate in a double-well potential. Our analysis hinges on the observation that such systems can be mapped onto an effective Schrödinger-like equation. This allows for detailed analytical calculations using a harmonic approximation of the local minima of the effective potential. As our main result, we showed that upon passing a quantum phase transition, the ground state of the system is characterized by strong Bell correlations that are extensive in  $N$ . We also showed the existence of the threshold temperature, above which the thermal noise dampens the Bell correlations.

For this work, the role of symmetry was crucial since the reduced dimensionality allows for high- $N$  simulations and for the Schrödinger-like equation approach. While for the two-mode BEC this symmetry is inherent, for a spin chain it requires all-to-all interactions [52]. Nevertheless, some of our analysis holds even if this condition is relaxed. For instance, when an initial product state evolves under the Ising-type

Hamiltonian

$$\hat{H} = - \sum_{i>j} J_{ij} \hat{\sigma}_z^{(i)} \hat{\sigma}_z^{(j)} + h \sum_i \hat{\sigma}_x^{(i)}, \quad (45)$$

the strength and depth of many-body correlations improve when the range of the distance-dependent interactions  $J_{ij}$  is high. However, even finite-range interactions lead to the creation of many-body Bell correlations [82]. Also, the ground state of the Hamiltonian (45) for  $h = 0$  is the desired GHZ state, disregarding the form of  $J_{ij}$ . For the nearest-neighbor case,  $J_{ij} \propto \delta_{i,i+1}$ , the system undergoes a QPT at  $h = -1$ , where the entanglement depth related to the GHZ type of coherence grows rapidly [62,63,84].

With the expected advent of NISQ devices, such a precisely tailored analysis might help to solve various theoretical and

experimental problems, particularly in the context of MBQC. Nevertheless, our understanding of how many-body Bell correlations can be used as a resource for modern quantum technologies is still *in statu nascendi*. A seminal work on quantum cryptography [85] and a more recent perspective on quantum metrology [32] can serve as examples.

## ACKNOWLEDGMENTS

This project was funded by the National Science Centre, Poland, within the QuantERA II Programme, which has received funding from the European Union's Horizon 2020 research and innovation program under Grant Agreement No. 101017733, Project No. 2021/03/Y/ST2/00195.

- 
- [1] A. Einstein, B. Podolsky, and N. Rosen, Can quantum-mechanical description of physical reality be considered complete? *Phys. Rev.* **47**, 777 (1935).
- [2] J. S. Bell, On the Einstein Podolsky Rosen paradox, *Phys. Phys. Fiz.* **1**, 195 (1964).
- [3] J. F. Clauser, M. A. Horne, A. Shimony, and R. A. Holt, Proposed experiment to test local hidden-variable theories, *Phys. Rev. Lett.* **23**, 880 (1969).
- [4] S. J. Freedman and J. F. Clauser, Experimental test of local hidden-variable theories, *Phys. Rev. Lett.* **28**, 938 (1972).
- [5] A. Aspect, P. Grangier, and G. Roger, Experimental tests of realistic local theories via Bell's theorem, *Phys. Rev. Lett.* **47**, 460 (1981).
- [6] A. Aspect, J. Dalibard, and G. Roger, Experimental test of Bell's inequalities using time-varying analyzers, *Phys. Rev. Lett.* **49**, 1804 (1982).
- [7] W. Tittel, J. Brendel, B. Gisin, T. Herzog, H. Zbinden, and N. Gisin, Experimental demonstration of quantum correlations over more than 10 km, *Phys. Rev. A* **57**, 3229 (1998).
- [8] W. Tittel, J. Brendel, H. Zbinden, and N. Gisin, Violation of Bell inequalities by photons more than 10 km apart, *Phys. Rev. Lett.* **81**, 3563 (1998).
- [9] G. Weihs, T. Jennewein, C. Simon, H. Weinfurter, and A. Zeilinger, Violation of Bell's inequality under strict Einstein locality conditions, *Phys. Rev. Lett.* **81**, 5039 (1998).
- [10] J.-W. Pan, D. Bouwmeester, M. Daniell, H. Weinfurter, and A. Zeilinger, Experimental test of quantum nonlocality in three-photon Greenberger-Horne-Zeilinger entanglement, *Nature (London)* **403**, 515 (2000).
- [11] M. A. Rowe, D. Kielpinski, V. Meyer, C. A. Sackett, W. M. Itano, C. Monroe, and D. J. Wineland, Experimental violation of a Bell's inequality with efficient detection, *Nature (London)* **409**, 791 (2001).
- [12] S. Gröblacher, T. Paterek, R. Kaltenbaek, Č. Brukner, M. Żukowski, M. Aspelmeyer, and A. Zeilinger, An experimental test of non-local realism, *Nature (London)* **446**, 871 (2007).
- [13] D. Salart, A. Baas, J. A. W. van Houwelingen, N. Gisin, and H. Zbinden, Spacelike separation in a Bell test assuming gravitationally induced collapses, *Phys. Rev. Lett.* **100**, 220404 (2008).
- [14] M. Ansmann, H. Wang, R. C. Bialczak, M. Hofheinz, E. Lucero, M. Neeley, A. D. O'Connell, D. Sank, M. Weides, J. Wenner, A. N. Cleland, and J. M. Martinis, Violation of Bell's inequality in Josephson phase qubits, *Nature (London)* **461**, 504 (2009).
- [15] M. Giustina, A. Mech, S. Ramelow, B. Wittmann, J. Kofler, J. Beyer, A. Lita, B. Calkins, T. Gerrits, S. W. Nam, R. Ursin, and A. Zeilinger, Bell violation using entangled photons without the fair-sampling assumption, *Nature (London)* **497**, 227 (2013).
- [16] B. Hensen *et al.*, Loophole-free Bell inequality violation using electron spins separated by 1.3 kilometres, *Nature (London)* **526**, 682 (2015).
- [17] E. Schrödinger, Die gegenwärtige situation in der quantenmechanik, *Naturwissenschaften* **23**, 807 (1935).
- [18] R. Horodecki, P. Horodecki, M. Horodecki, and K. Horodecki, Quantum entanglement, *Rev. Mod. Phys.* **81**, 865 (2009).
- [19] M. D. Reid, P. D. Drummond, W. P. Bowen, E. G. Cavalcanti, P. K. Lam, H. A. Bachor, U. L. Andersen, and G. Leuchs, Colloquium: The Einstein-Podolsky-Rosen paradox: From concepts to applications, *Rev. Mod. Phys.* **81**, 1727 (2009).
- [20] B. Yadin, M. Fadel, and M. Gessner, Metrological complementarity reveals the Einstein-Podolsky-Rosen paradox, *Nat. Commun.* **12**, 1 (2021).
- [21] R. Raussendorf, D. E. Browne, and H. J. Briegel, Measurement-based quantum computation on cluster states, *Phys. Rev. A* **68**, 022312 (2003).
- [22] D. W. Leung, Quantum computation by measurements, *Int. J. Quantum Inf.* **02**, 33 (2004).
- [23] R. Jozsa, An introduction to measurement based quantum computation, *Quantum Information Processing: From Theory to Experiment*, NATO Science Series, III: Computer and Systems Sciences (IOS Press, Amsterdam, 2006), Vol. 199, p. 137.
- [24] D. Gross and J. Eisert, Novel schemes for measurement-based quantum computation, *Phys. Rev. Lett.* **98**, 220503 (2007).
- [25] H. J. Briegel, D. E. Browne, W. Dür, R. Raussendorf, and M. Van den Nest, Measurement-based quantum computation, *Nat. Phys.* **5**, 19 (2009).
- [26] R. Raussendorf and T.-C. Wei, Quantum computation by local measurement, *Annu. Rev. Condens. Matter Phys.* **3**, 239 (2012).
- [27] M. Frembs, S. Roberts, E. T. Campbell, and S. D. Bartlett, Hierarchies of resources for measurement-based quantum computation, *New J. Phys.* **25**, 013002 (2023).
- [28] N. D. Mermin, Extreme quantum entanglement in a superposition of macroscopically distinct states, *Phys. Rev. Lett.* **65**, 1838 (1990).



- [29] Q. Y. He, E. G. Cavalcanti, M. D. Reid, and P. D. Drummond, Bell inequalities for continuous-variable measurements, *Phys. Rev. A* **81**, 062106 (2010).
- [30] Q. Y. He, P. D. Drummond, and M. D. Reid, Entanglement, EPR steering, and Bell-nonlocality criteria for multipartite higher-spin systems, *Phys. Rev. A* **83**, 032120 (2011).
- [31] E. G. Cavalcanti, S. J. Jones, H. M. Wiseman, and M. D. Reid, Experimental criteria for steering and the Einstein-Podolsky-Rosen paradox, *Phys. Rev. A* **80**, 032112 (2009).
- [32] A. Niezgodá and J. Chwedeñczuk, Many-body nonlocality as a resource for quantum-enhanced metrology, *Phys. Rev. Lett.* **126**, 210506 (2021).
- [33] M. Kitagawa and M. Ueda, Squeezed spin states, *Phys. Rev. A* **47**, 5138 (1993).
- [34] D. J. Wineland, J. J. Bollinger, W. M. Itano, and D. J. Heinzen, Squeezed atomic states and projection noise in spectroscopy, *Phys. Rev. A* **50**, 67 (1994).
- [35] J. Esteve, C. Gross, A. Weller, S. Giovanazzi, and M. Oberthaler, Squeezing and entanglement in a Bose-Einstein condensate, *Nature (London)* **455**, 1216 (2008).
- [36] J. Appel, P. J. Windpassinger, D. Oblak, U. B. Hoff, N. Kjærgaard, and E. S. Polzik, Mesoscopic atomic entanglement for precision measurements beyond the standard quantum limit, *Proc. Natl. Acad. Sci. USA* **106**, 10960 (2009).
- [37] L. Pezzé and A. Smerzi, Entanglement, nonlinear dynamics, and the Heisenberg limit, *Phys. Rev. Lett.* **102**, 100401 (2009).
- [38] M. F. Riedel, P. Böhi, Y. Li, T. W. Hänsch, A. Sinatra, and P. Treutlein, Atom-chip-based generation of entanglement for quantum metrology, *Nature (London)* **464**, 1170 (2010).
- [39] C. Gross, T. Zibold, E. Nicklas, J. Estève, and M. K. Oberthaler, Nonlinear atom interferometer surpasses classical precision limit, *Nature (London)* **464**, 1165 (2010).
- [40] T. Berrada, S. van Frank, R. Bücker, T. Schumm, J.-F. Schaff, and J. Schmiedmayer, Integrated Mach-Zehnder interferometer for Bose-Einstein condensates, *Nat. Commun.* **4**, 2077 (2013).
- [41] L. Pezze, A. Smerzi, M. K. Oberthaler, R. Schmied, and P. Treutlein, Quantum metrology with nonclassical states of atomic ensembles, *Rev. Mod. Phys.* **90**, 035005 (2018).
- [42] J. Tura, R. Augusiak, A. B. Sainz, T. Vértesi, M. Lewenstein, and A. Acín, Detecting nonlocality in many-body quantum states, *Science* **344**, 1256 (2014).
- [43] R. Schmied, J.-D. Bancal, B. Allard, M. Fadel, V. Scarani, P. Treutlein, and N. Sangouard, Bell correlations in a Bose-Einstein condensate, *Science* **352**, 441 (2016).
- [44] A. Niezgodá, J. Chwedeñczuk, L. Pezzé, and A. Smerzi, Detection of Bell correlations at finite temperature from matter-wave interference fringes, *Phys. Rev. A* **99**, 062115 (2019).
- [45] R. Blatt and C. F. Roos, Quantum simulations with trapped ions, *Nat. Phys.* **8**, 277 (2012).
- [46] J. Zhang, G. Pagano, P. W. Hess, A. Kyprianidis, P. Becker, H. Kaplan, A. V. Gorshkov, Z.-X. Gong, and C. Monroe, Observation of a many-body dynamical phase transition with a 53-qubit quantum simulator, *Nature (London)* **551**, 601 (2017).
- [47] C. Monroe, W. C. Campbell, L.-M. Duan, Z.-X. Gong, A. V. Gorshkov, P. W. Hess, R. Islam, K. Kim, N. M. Linke, G. Pagano, P. Richerme, C. Senko, and N. Y. Yao, Programmable quantum simulations of spin systems with trapped ions, *Rev. Mod. Phys.* **93**, 025001 (2021).
- [48] M. K. Joshi, F. Kranzl, A. Schuckert, I. Lovas, C. Maier, R. Blatt, M. Knapp, and C. F. Roos, Observing emergent hydrodynamics in a long-range quantum magnet, *Science* **376**, 720 (2022).
- [49] W. Morong, F. Liu, P. Becker, K. Collins, L. Feng, A. Kyprianidis, G. Pagano, T. You, A. Gorshkov, and C. Monroe, Observation of Stark many-body localization without disorder, *Nature (London)* **599**, 393 (2021).
- [50] P. T. Dumitrescu, J. G. Bohnet, J. P. Gaebler, A. Hankin, D. Hayes, A. Kumar, B. Neyenhuis, R. Vasseur, and A. C. Potter, Dynamical topological phase realized in a trapped-ion quantum simulator, *Nature (London)* **607**, 463 (2022).
- [51] L. Feng, O. Katz, C. Haack, M. Maghrebi, A. V. Gorshkov, Z. Gong, M. Cetina, and C. Monroe, Continuous symmetry breaking in a trapped-ion spin chain, *Nature (London)* **623**, 713 (2023).
- [52] M. Pita-Vidal, J. J. Wesdorp, and C. K. Andersen, Blueprint for all-to-all connected superconducting spin qubits, *arXiv:2405.09988*.
- [53] G.-B. Jo, Y. Shin, S. Will, T. Pasquini, M. Saba, W. Ketterle, D. E. Pritchard, M. Vengalattore, and M. Prentiss, Long phase coherence time and number squeezing of two Bose-Einstein condensates on an atom chip, *Phys. Rev. Lett.* **98**, 030407 (2007).
- [54] W. Hofstetter and T. Qin, Quantum simulation of strongly correlated condensed matter systems, *J. Phys. B* **51**, 082001 (2018).
- [55] T. Hernández Yanes, M. Płodzień, M. Mackoít Sinkevičienė, G. Žlabys, G. Juzeliūnas, and E. Witkowska, One- and two-axis squeezing via laser coupling in an atomic Fermi-Hubbard model, *Phys. Rev. Lett.* **129**, 090403 (2022).
- [56] T. Schumm, S. Hofferberth, L. M. Andersson, S. Wildermuth, S. Groth, I. Bar-Joseph, J. Schmiedmayer, and P. Krüger, Matter-wave interferometry in a double well on an atom chip, *Nat. Phys.* **1**, 57 (2005).
- [57] M. Dziurawiec, T. Hernández Yanes, M. Płodzień, M. Gajda, M. Lewenstein, and E. Witkowska, Accelerating many-body entanglement generation by dipolar interactions in the Bose-Hubbard model, *Phys. Rev. A* **107**, 013311 (2023).
- [58] K. Pawłowski, M. Fadel, P. Treutlein, Y. Castin, and A. Sinatra, Mesoscopic quantum superpositions in bimodal Bose-Einstein condensates: Decoherence and strategies to counteract it, *Phys. Rev. A* **95**, 063609 (2017).
- [59] R. Gati, B. Hemmerling, J. Fölling, M. Albiez, and M. K. Oberthaler, Noise thermometry with two weakly coupled Bose-Einstein condensates, *Phys. Rev. Lett.* **96**, 130404 (2006).
- [60] J. Dziarmaga, A. Smerzi, W. H. Zurek, and A. R. Bishop, Dynamics of quantum phase transition in an array of Josephson junctions, *Phys. Rev. Lett.* **88**, 167001 (2002).
- [61] A. Trenkwalder *et al.*, Quantum phase transitions with parity-symmetry breaking and hysteresis, *Nat. Phys.* **12**, 826 (2016).
- [62] C. Invernizzi, M. Korbman, L. Campos Venuti, and M. G. A. Paris, Optimal quantum estimation in spin systems at criticality, *Phys. Rev. A* **78**, 042106 (2008).
- [63] P. Zanardi, M. G. A. Paris, and L. Campos Venuti, Quantum criticality as a resource for quantum estimation, *Phys. Rev. A* **78**, 042105 (2008).
- [64] G. Salvatori, A. Mandarino, and M. G. A. Paris, Quantum metrology in Lipkin-Meshkov-Glick critical systems, *Phys. Rev. A* **90**, 022111 (2014).
- [65] M. Bina, I. Amelio, and M. G. A. Paris, Dicke coupling by feasible local measurements at the superradiant quantum phase transition, *Phys. Rev. E* **93**, 052118 (2016).

- [66] L. Garbe, M. Bina, A. Keller, M. G. A. Paris, and S. Felicetti, Critical quantum metrology with a finite-component quantum phase transition, *Phys. Rev. Lett.* **124**, 120504 (2020).
- [67] A. Piga, A. Aloy, M. Lewenstein, and I. Frérot, Bell correlations at Ising quantum critical points, *Phys. Rev. Lett.* **123**, 170604 (2019).
- [68] O. Gühne, G. Tóth, and H. J. Briegel, Multipartite entanglement in spin chains, *New J. Phys.* **7**, 229 (2005).
- [69] G. Tóth and I. Apellaniz, Quantum metrology from a quantum information science perspective, *J. Phys. A* **47**, 424006 (2014).
- [70] F. Iglói and G. Tóth, Entanglement witnesses in the  $xy$  chain: Thermal equilibrium and postquench nonequilibrium states, *Phys. Rev. Res.* **5**, 013158 (2023).
- [71] P. Ziń, J. Chwedeńczuk, B. Oleś, K. Sacha, and M. Trippenbach, Critical fluctuations of an attractive Bose gas in a double-well potential, *Europhys. Lett.* **83**, 64007 (2008).
- [72] J. Chwedeńczuk, P. Hyllus, F. Piazza, and A. Smerzi, Sub-shot-noise interferometry from measurements of the one-body density, *New J. Phys.* **14**, 093001 (2012).
- [73] E. G. Cavalcanti, C. J. Foster, M. D. Reid, and P. D. Drummond, Bell inequalities for continuous-variable correlations, *Phys. Rev. Lett.* **99**, 210405 (2007).
- [74] E. G. Cavalcanti, Q. Y. He, M. D. Reid, and H. M. Wiseman, Unified criteria for multipartite quantum nonlocality, *Phys. Rev. A* **84**, 032115 (2011).
- [75] A. Niezgoda, M. Panfil, and J. Chwedeńczuk, Quantum correlations in spin chains, *Phys. Rev. A* **102**, 042206 (2020).
- [76] J. Chwedeńczuk, Many-body Bell inequalities for bosonic qubits, *SciPost Phys. Core* **5**, 025 (2022).
- [77] Note that at this stage the parities are not assumed to be restricted by quantum theory.
- [78] J. S. Bell, On the problem of hidden variables in quantum mechanics, *Rev. Mod. Phys.* **38**, 447 (1966).
- [79] N. Brunner, D. Cavalcanti, S. Pironio, V. Scarani, and S. Wehner, Bell nonlocality, *Rev. Mod. Phys.* **86**, 419 (2014).
- [80] M. Żukowski and Č. Brukner, Bell's theorem for general  $N$ -qubit states, *Phys. Rev. Lett.* **88**, 210401 (2002).
- [81] D. M. Greenberger, M. A. Horne, and A. Zeilinger, Going beyond Bell's theorem, *Bell's Theorem, Quantum Theory and Conceptions of the Universe* (Kluwer Academic Publishers, Dordrecht, Netherlands, 1989), pp. 69–72.
- [82] M. Płodzień, T. Wasak, E. Witkowska, M. Lewenstein, and J. Chwedeńczuk, Generation of scalable many-body bell correlations in spin chains with short-range two-body interactions, *Phys. Rev. Res.* **6**, 023050 (2024).
- [83] M. Płodzień, M. Lewenstein, E. Witkowska, and J. Chwedeńczuk, One-axis twisting as a method of generating many-body Bell correlations, *Phys. Rev. Lett.* **129**, 250402 (2022).
- [84] T. J. Osborne and M. A. Nielsen, Entanglement in a simple quantum phase transition, *Phys. Rev. A* **66**, 032110 (2002).
- [85] A. K. Ekert, Quantum cryptography based on Bell's theorem, *Phys. Rev. Lett.* **67**, 661 (1991).